JOURNAL OF Materials CHEMISTRY

Atomic force microscopy investigation of the surface modification of highly oriented pyrolytic graphite by oxygen plasma

Juan I. Paredes, Amelia Martínez-Alonso* and Juan M. D. Tascón

Instituto Nacional del Carbón, CSIC, La Corredoria s/n, Apartado 73, 33080 Oviedo, Spain

Received 25th January 2000, Accepted 6th April 2000
Published on the Web 30th May 2000

The surface modification of highly oriented pyrolytic graphite (HOPG) by a microwave oxygen plasma has been studied by means of atomic force microscopy. The purpose of this work is to investigate the interactions of a plasma with a model material, such as HOPG, in order to understand the basic processes that may also occur in other carbon-based materials of interest. The HOPG samples were treated under different experimental conditions and showed, in general, a smoothly roughened topography, as opposed to the atomically flat untreated samples, with observable differences for the various etching conditions. At low microwave powers, the samples develop a great number of isolated peaks, with typical sizes between 10 and 15 nm, that evolve into connected protuberances with increasing power. With extended etching times, the formation of pits of different sizes in localized areas reflects a strong tendency for the reaction to progress remarkably faster along defects in the surface. Pits can be found with a wide range of diameters, but the maximum diameters tend to increase with etching time; from 50 nm after 10 min to 75 and 120 nm after 15 and 20 min, respectively. The origin of the features can be explained by the chemical selectivity of atomic oxygen, the main reactive species in an oxygen plasma, which reacts with carbon atoms from both defect sites and basal planes (as opposed to molecular oxygen), but with a slightly different rate that leads to the reported observations.

1 Introduction

The interaction of surfaces of different materials with cold plasmas is of great interest, not only from the technological point of view, but also from a basic knowledge perspective. The surface reaction mechanisms of many plasma processes are not well understood or characterized experimentally, due to their extreme complexity.[1] In many cases, the modifications induced by the plasma are desirable, since they can improve the properties, such as adhesion, wettability, roughness, lubricity, conductivity, *etc*., of materials with applications in biomedicine, microelectronics or thin-film technology.[2,3]

On the other hand, there are certain situations in which the action of some of the species generated in a plasma has rather negative effects, resulting in damage to the surface of the material, which in turn reduces its durability. For instance, the construction materials of shuttle flights are exposed to atomic oxygen (the dominant reactive species in an oxygen plasma) at altitudes between 200 and 700 km, with important consequences for their performance and durability.[4,5] Another example can be found in graphite or other carbon-based materials, used as first-wall material in thermonuclear fusion devices,[6,7] where they are subjected to an important material deterioration due to high energy ion bombardment and to the oxygen present as an impurity in the fusion plasma.[8,9]

In this context, the study of the etching mechanisms of highly oriented pyrolytic graphite (HOPG) in oxygen plasmas has a special relevance, not only because of its specific applications, but also owing to its status as a model material. As an example, patterning of HOPG by oxygen plasma etching has been reported very recently,[10] with the aim of developing novel nanodevices by assembling carbon by design.

The study of the physical and chemical properties of the modified surface of graphite, not only by plasmas, but also by other kinds of treatments, such as electrochemical, thermal or wet chemical oxidation and ion or cluster bombardment, has been carried out by means of a variety of analytical techniques, including X-ray photoelectron spectroscopy (XPS),[11] Fourier transform infrared attenuated total reflection spectroscopy (FT-IR-ATR),[11,12] high resolution electron energy loss spectroscopy (HREELS),[13] temperature programmed desorption (TPD),[13] ac impedance spectroscopy,[14] scanning and transmission electron microscopy (SEM/TEM)[14,15] and, more recently, scanning tunneling microscopy and spectroscopy (STM/STS)[13,16–30] and atomic force microscopy (AFM).[29–32]

In the work presented here, atomic force microscopy has been used to study the etching mechanisms of highly oriented pyrolytic graphite in an oxygen plasma generated by microwave (MW) radiation under different experimental conditions. To the authors' knowledge, there have been no reports of detailed AFM work on the surface modification of HOPG following MW oxygen plasma etching, though there is some published work on this type of modification on polymers.[33]

2 Experimental

Fresh surfaces of HOPG (Union Carbide, grade ZYH) were prepared by cleaving in air with adhesive tape. The samples were immediately placed in a Technics Plasma 200-G treatment chamber where an oxygen plasma was generated using 2.45 GHz microwave radiation. The microwave field was generated by means of a magnetron, and a waveguide was employed to transfer microwave power between this source and the point of use, which was a quartz reactor (batch type) where the plasma was created and the samples were placed. A dielectric window connected the waveguide with the quartz reactor. The oxygen pressure in the chamber during the etching was kept at 1.0 mbar (0.7 Torr).

Two kinds of experiments were carried out in this work. In the first, the etching time was kept constant (5 min) and different samples were treated at MW powers of 50, 100 and 250 W. In the other, the exposure time was varied from 5 to 10, 15 and 20 min and the MW power was kept constant at 100 W. In order to achieve results which are as reproducible as possible, all the samples were placed in the chamber in the same fashion, that is, with the sample surface facing the dielectric window at a fixed distance.

After treatment, the samples were studied by AFM in air at room temperature with a Nanoscope Multimode IIIa microscope from Digital Instruments (D.I.). Measurements were made in contact mode as well as in tapping mode.[34,35] In the former, microfabricated Si_3N_4 cantilevers (D.I.) with a spring constant of 0.06 N m^{-1} and a tip radius of curvature of 20–60 nm were used. The cantilevers used for tapping mode, also from D.I., were made of etched silicon and had a nominal tip radius of curvature of 5–10 nm.

In the case of the HOPG samples studied by tapping mode, special care was taken to minimize the tip–sample interaction, which is necessary in order to obtain accurate surface topographic information.[36] Likewise, the repulsive force in contact mode was kept to a minimum. It was observed that the images obtained in tapping mode were practically always of a higher quality than the ones obtained in contact mode. In the latter case, the tip-induced changes on the sample were apparent after several consecutive scans over the same area. This led to "smeared out" features and, generally, to unsatisfactory images with rather poor resolution. In some cases, a physical movement of material from the sample surface was also evident, presumably dragged along by the tip. On the other hand, the images obtained in tapping mode showed features with improved resolution, were reproducible and did not degrade after several consecutive scans. This different behaviour is due to the fact that in contact mode the capillary condensation between tip and sample gives rise to high compressive and shear lateral forces, whereas in tapping mode the cantilever is oscillated at an amplitude high enough to overcome the capillary condensation forces, greatly reducing the lateral shear forces and allowing for a lower disruption of the surface. This, combined with the smaller tip radius, results in better resolution, as compared to that of the contact mode. From this, one can conclude that the plasma-modified surfaces of HOPG are, in general, too soft to be imaged by contact mode and it is for this reason that all the images presented in this work were obtained in tapping mode, except for one low resolution contact mode image showing features big enough for this mode to be sufficiently accurate. Likewise, to validate the reproducibility of the AFM images and check that the observed features were not a consequence of tip artifacts, most of the samples were studied with at least two different previously unused tips and, in many cases, the images were obtained by scanning along different directions. The images shown in this work are representative of the studied surfaces and were obtained in several different areas of each sample. To improve their visual presentation, the images were subjected to a flattening and then were smoothed by a single application of a low-pass filter. Care was taken to ensure that no distortion or artifacts were introduced.

3 Results

The fresh HOPG surfaces show large atomically flat areas along with defects and discontinuities, such as steps, grain borders or dislocations. In contrast to this, a common characteristic of the plasma-treated samples was the presence of a rough topography with nanometer-sized hillocks spreading all over the previously atomically flat surfaces. Fig. 1 shows typical images of pristine and etched samples (at a MW power of 250 W for 5 min) in which the aforementioned differences are already obvious. In Fig. 1a, the occurrence of several atomically flat planes at different heights is a consequence of the cleaving process, which prevents the obtention of a single atomically flat one.

Fig. 2 compares the typical detailed topography encountered in the samples treated in oxygen plasma for 5 min at MW powers of 50 (a), 100 (b) and 250 W (c). At the lowest power used (50 W), the surface consists of a large number of hillocks

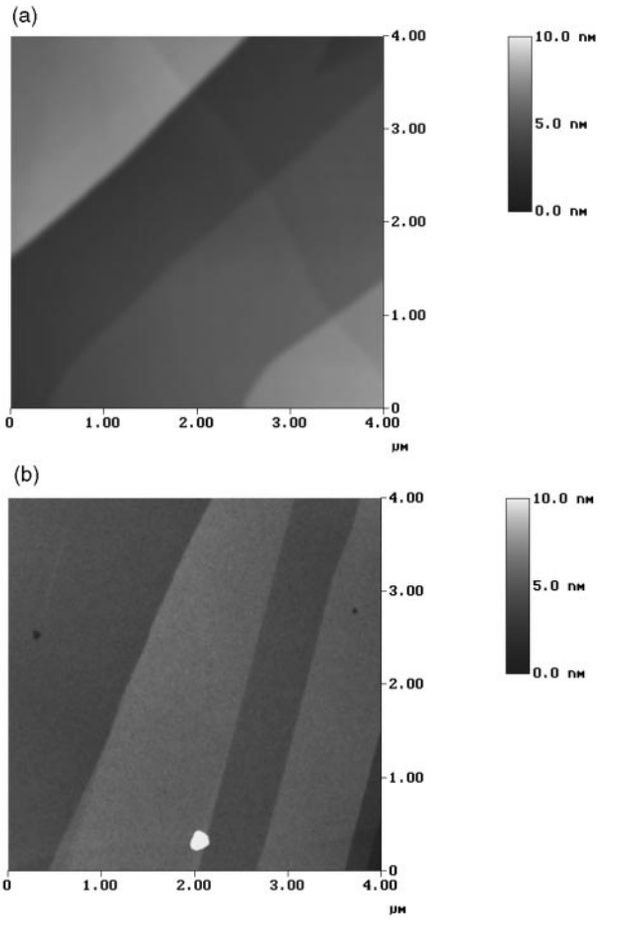

Fig. 1 Typical AFM images of the HOPG surface, untreated (a) and treated in a MW oxygen plasma at a power of 250 W for 5 min (b). The scan size is 4 μm.

(with lateral dimensions of 10–15 nm) surrounded by lower areas, in an apparently random arrangement. These hillocks gradually disappear or become more rounded when the plasma power is increased (100 W) and eventually at the highest power used, *i.e.* 250 W, they evolve into protuberances which are connected to each other and with no clear isolated peaks (as was the case with the 50 W sample), but with more even tops instead. The height differences between the tops of the hills and the bottoms of the valleys are approximately the same (1–2 nm) in the three samples, but tending to decrease slightly with increasing plasma power. Scans of a smaller size than those presented in Fig. 2 (see below) did not reveal new surface features, indicating that the tapping mode was near its resolution limit for this type of sample.

In order to quantitatively compare the height of the features in the samples at these different etching powers, height histograms were drawn (Fig. 3) by representing the percentage of pixels the images have for every height range. To facilitate the comparison at the three power levels used, the enveloping curve of every histogram is given. The lowest-lying point of every image is always taken as zero height, so that all heights are referred to that point. When the three histograms are compared, several general features consistent with the aforementioned observations can be seen. Firstly, when the MW power is increased, the curves tend to narrow and their maximum values tend to rise. This is due to the fact that, at increasing powers, the hillocks begin to connect with each other, as seen in the images in Fig. 2, so the surface points tend to have more similar heights to those of their neighbours, leading to slightly narrower histograms with higher maxima. Secondly, narrower histograms imply, in general, smaller height differences between high and low-lying points on the

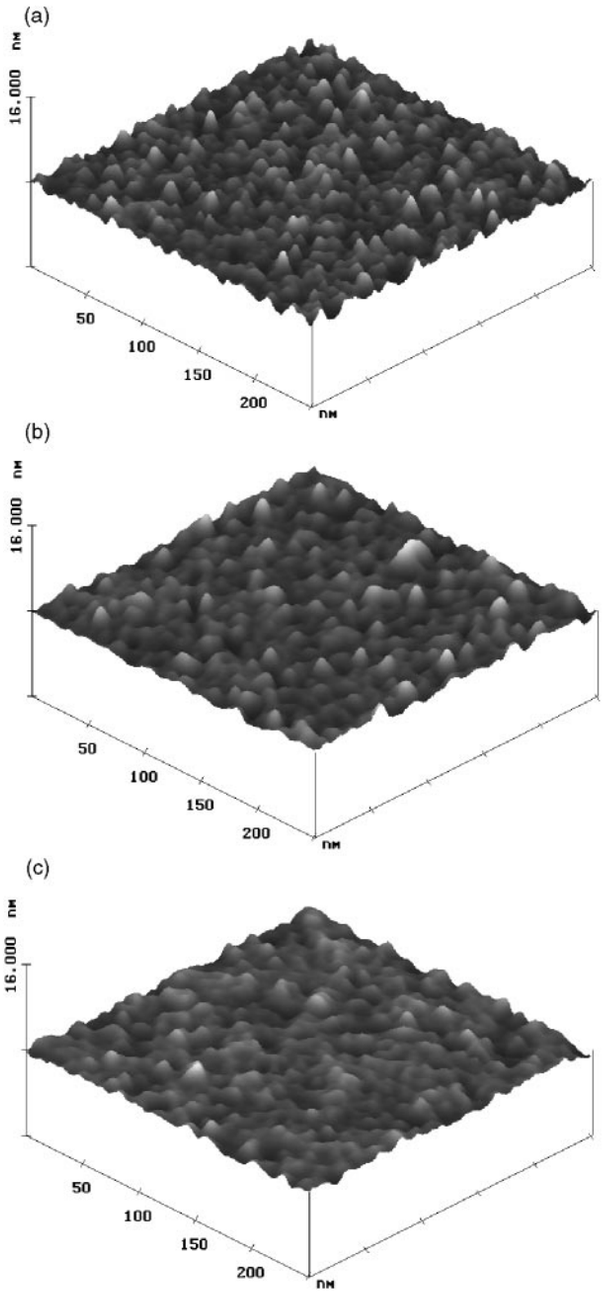

Fig. 2 Three-dimensional AFM images of HOPG samples treated in a MW oxygen plasma for 5 min at powers of 50 (a), 100 (b) and 250 W (c). The scan size is 250 nm.

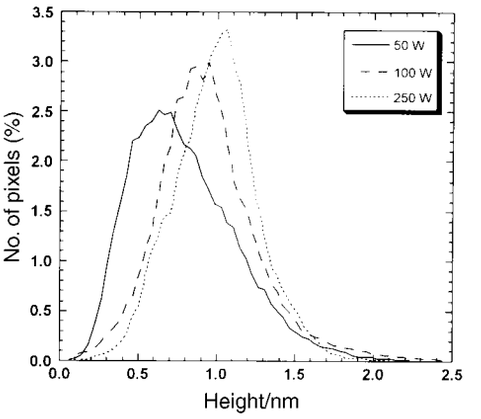

Fig. 3 Height histograms of HOPG surfaces treated in a MW oxygen plasma for 5 min at different power levels.

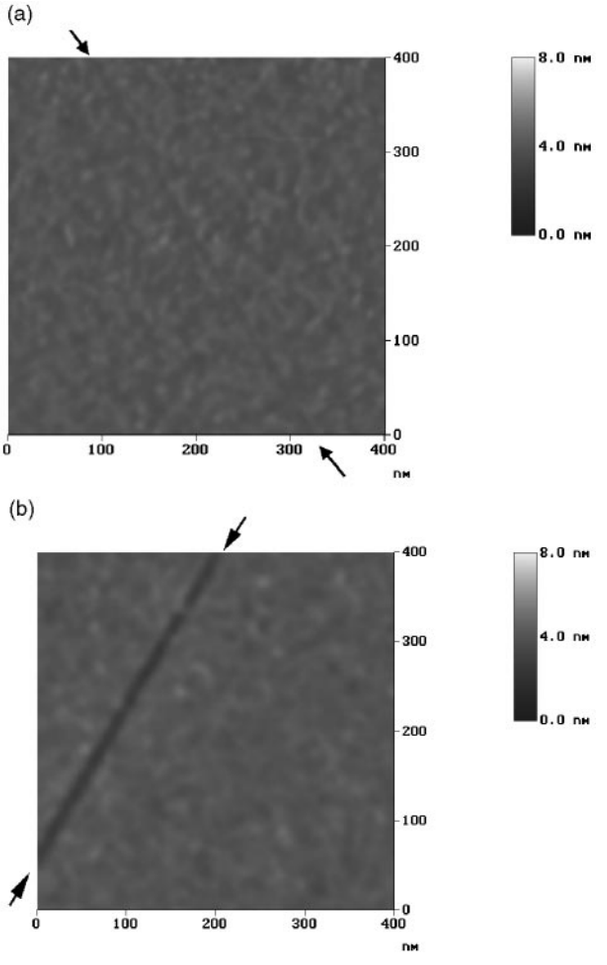

Fig. 4 AFM images showing the development of grooves in plasma treated samples at powers of 50 (a) and 100 W (b) for 5 min. The scan size is 400 nm.

surface, as mentioned previously. It can also be seen that the most frequent height values tend to increase slightly with power, a consequence of the narrowing of the valleys that leads to connections between hillocks. Thirdly, the histogram at a power of 50 W presents a tail at high height values, arising from the abundant isolated peaks of the hillocks observed in the corresponding three-dimensional image in Fig. 2. These isolated peaks tend to disappear with increasing MW powers, thus explaining the attenuation of the tails at 100 and 250 W.

Along with the general topography of the samples treated at different powers, other features were also found. As an example, Fig. 4 shows images of grooves encountered occasionally in the samples treated at 50 W (a) and 100 W (b). Similar grooves were also found in the 250 W sample. These grooves are 0.7 nm deep and 8 nm wide for the 50 W sample, seeming to be at a very early stage of formation, and 1.4 nm deep, 15 nm wide for the 100 W sample. The depth and width for the grooves encountered in the 250 W sample were typically 2 and 70 nm, respectively. This evidences a clear tendency for the formation of deeper and, especially, wider grooves with increasing power.

Fig. 5 shows the topographical evolution of the HOPG samples with plasma etching time for a constant MW power (100 W). It is interesting to note the formation of pits in the surface which grow deeper and wider with longer exposures to the plasma. After a treatment time of 5 min, there are no clearly observable pits formed on the surface, but after 10 min some pits begin to appear, having typical depths of 1–2 nm and

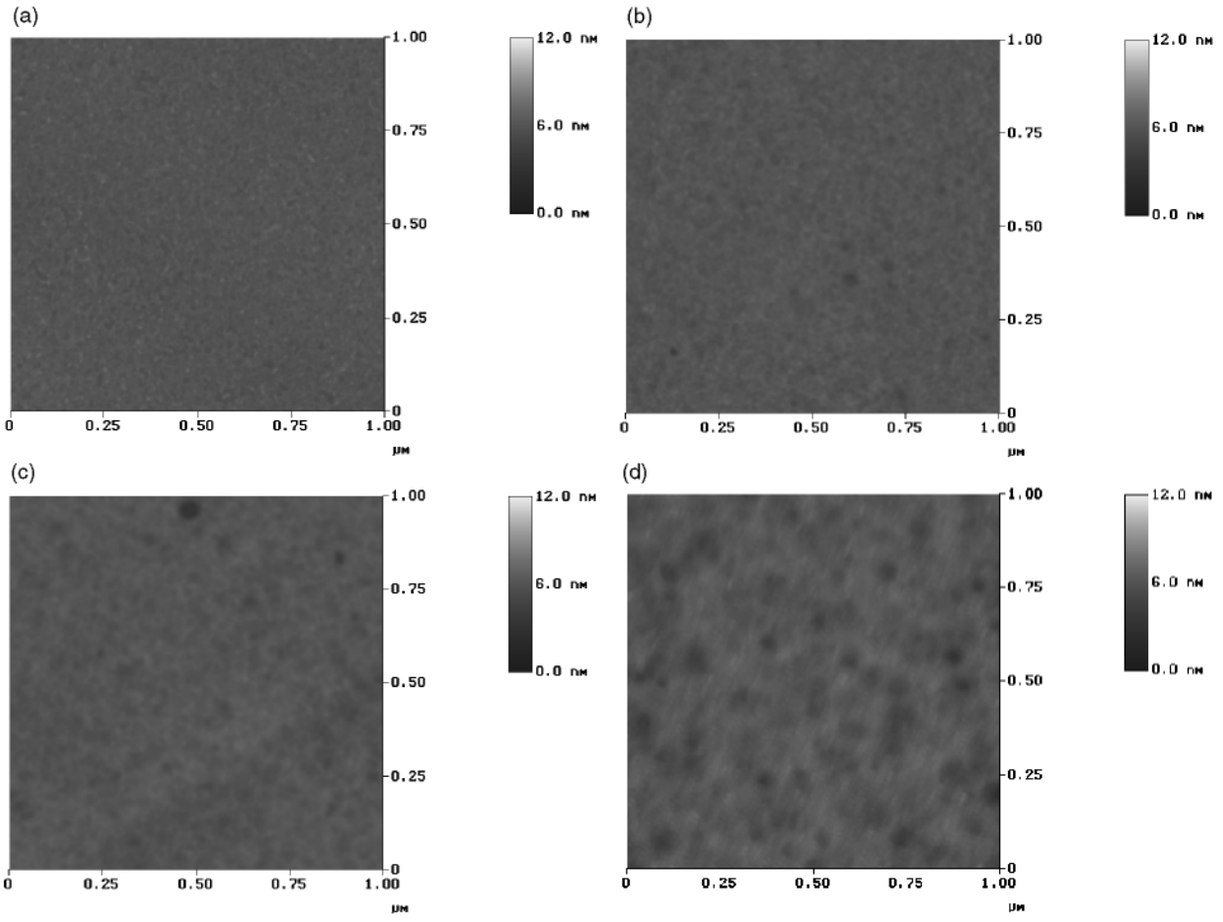

Fig. 5 1×1 μm AFM images showing the evolution of topography with plasma etching time. (a) 5, (b) 10, (c) 15 and (d) 20 min. The MW plasma power was kept at a constant value of 100 W.

diameters between 25 and 50 nm. When the etching time is increased to 15 min, the pits have a depth of 1–3 nm and a diameter of 25–75 nm. Finally, when the samples are exposed for 20 min, the pits are much more abundant and they are typically 1–4 nm deep and 25–120 nm in diameter. From these results, an increase in the maximum diameter of the pits with etching time can be observed, although there are pits with a small diameter, *i.e.* 25 nm, in the samples treated for 15 and 20 min. Likewise, in all the samples, the depth of the pits is always much smaller than their diameter, implying that the etching is faster in the directions parallel to the basal plane than in the direction of the *c* axis. It could be argued that the AFM tip cannot reach the bottom of the pits due to its finite size and thus no conclusions about the speed of etching along the *c* axis direction can be drawn. However, considering the morphology and dimensions of the tapping mode tips used, this possibility can be ruled out, since the diameter of the observed pits allows for considerably deeper tip penetrations than the measured 1–4 nm.

Height histograms of the HOPG surfaces treated for different times are presented in Fig. 6. They show a displacement of the curves to higher values with increasing treatment time. Also, the curve corresponding to a treatment of 20 min is wider than the others. These two facts can be explained by the formation of an increasing number of pits with increasing depths in the HOPG surface with longer etching times, so that the zero height is well below the typical height values and its range gets wider.

Fig. 7 shows another typical feature of the sample treated for 20 min. It is observed that wherever there is unevenness on the surface, such as steps arising from the edges of basal planes, as is the case with this image, the etching progresses more rapidly

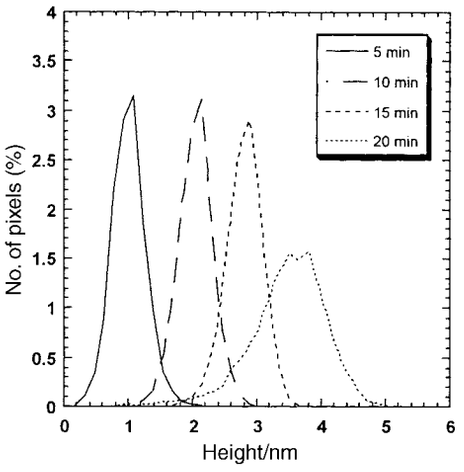

Fig. 6 Height histograms of HOPG surfaces treated in a MW oxygen plasma at a power of 100 W for different times.

than in perfect basal plane areas. This greater degree of etching manifests itself in the formation of pits all along the steps. These pits range in size and, apparently, have a random distribution along the steps.

Finally, Fig. 8(a) presents a low-resolution contact AFM image from the 20 min sample, showing some of the features mentioned previously, such as the pits formed on the basal planes. Because of the size of the scan, only the biggest pits can be appreciated in this image. On the other hand, the rapid development of pits at the edges of the basal planes can also be observed. In addition, this and similar images apparently

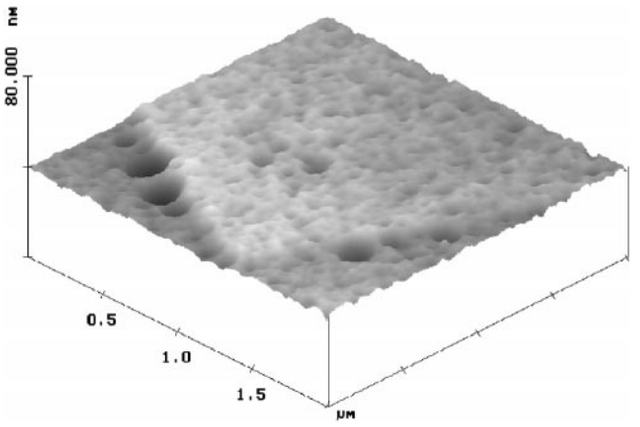

Fig. 7 AFM image of the 100 W, 20 min sample, showing the preferential formation of pits along steps on the HOPG surface. The scan size is 2 μm.

indicate that the higher the step is, the faster the pits develop. For instance, the step running along the bottom left part of the image shows a great number of nearly overlapping pits, whereas the much smaller steps running more or less parallel to the former have a much more limited number of pits. A section of the former along the line indicated by the arrows is presented in Fig. 8(b), showing the profile of a pit formed on the step. These pits have a depth between 4 and 15 nm and a diameter of 140–180 nm, which indicates again a preferential attack parallel to the basal plane. Though the profile shows evidence of some convolution between the tip and the pit walls, again in this case the pit depth is accurately determined since its diameter allows much deeper tip penetration than 4–15 nm.

4 Discussion

When a sample material is exposed to a plasma, a series of complex chemical and physical processes takes place on the sample surface,[1] the two most important being: (i) the combination of the sample surface atoms, carbon atoms in the case of HOPG, with the chemically active species present in the plasma (neutral atomic oxygen in an oxygen discharge) to form functional groups which eventually desorb as volatile reaction products, and (ii) an energetic ion bombardment arising from the different mobility of electrons and ions in the plasma, leading to the formation of a bias voltage between plasma and surface which accelerates the positive ions towards the specimen surface.[37] Chemical etching is an isotropic, non-directional process, since the reactive species reach the surface from random directions, whereas the ion bombardment is, in general, an anisotropic directional process. The physical effects of this bombardment will depend on the mass, flux and energy of the impinging ions, but it is generally accepted that one of its consequences is an increase in the etch rates, due to a synergistic effect between neutral chemical etchants and ion bombardment.[37–41]

Another question that should be borne in mind is the magnitude that this bombardment has in a particular plasma configuration. In the case of a radio-frequency (RF) oxygen plasma operating at a pressure of 20 mTorr, You *et al.*[16] showed the importance of the physical effects on the resulting topography of graphite. Nevertheless, in the present work, the oxygen plasma was generated by microwave radiation, which leads to chemical results that differ significantly from lower frequency plasmas.[42] Wertheimer and Moisan attribute these differences to different electron energy distribution functions. Likewise, in a MW plasma, the bias developed between plasma and substrate is much smaller than that of RF plasmas and the energy of ions impinging the substrate is typically 10–20 eV,[43] which is well below the minimum energy necessary to create

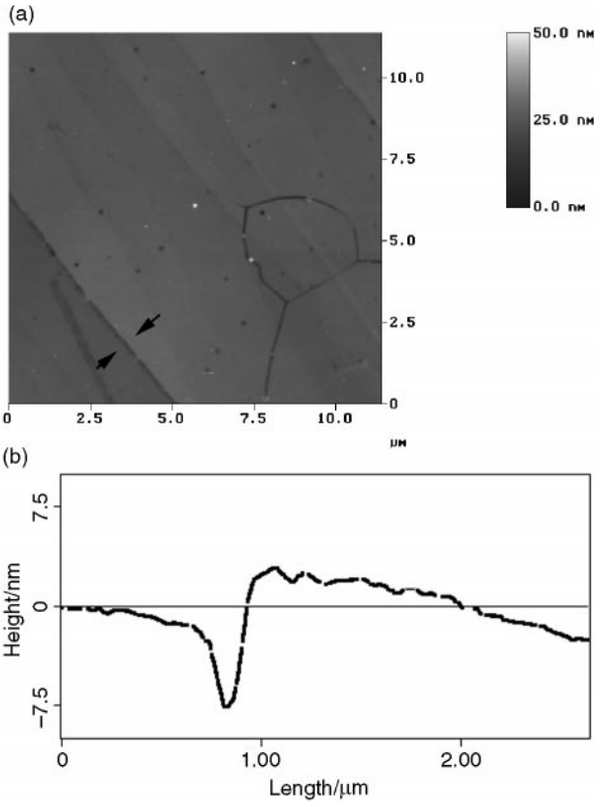

Fig. 8 (a) 11.4 × 11.4 μm contact AFM image of the sample treated at 100 W for 20 min; (b) section of the area indicated by arrows, showing the profile of a pit developed by a step.

stable defects on graphite, known as the displacement energy, which is $E_d = 34.5$ eV.[44] Thus, in this case, the ion bombardment plays a minor role in the etching of graphite and chemical reactions between the neutral species in the plasma and the substrate dominate the process.

As opposed to molecular oxygen, which only reacts with defects and discontinuities of the HOPG surface, such as atomic vacancies and steps,[19,24] the atomic oxygen present in an oxygen plasma reacts with carbon atoms from defects and discontinuities as well as from basal planes,[45] but due to the presence of highly reactive dangling bonds in defect areas, less-ordered carbon atoms have a higher probability of reacting with atomic oxygen than atoms in basal planes, which has been observed previously by other authors.[46] This chemical selectivity should lead to etching differences between defect areas and perfect sites of basal planes. Also, the differences generated by the plasma between defects and discontinuities and perfect areas in basal planes will be greater when the MW power is increased, as there is a higher density of reactive species in the plasma with increasing power.[47] However, as the atoms from defects have, *a priori*, a greater probability of reacting with the oxygen, the number of atoms subtracted from defects will increase to a greater extent than that from perfect sites in basal planes. The same argument can be applied when the etching time is increased. Thus, the dimensions of the pits and grooves that are created along defects should grow bigger with both increasing MW power and etching time. This can be appreciated in the images shown in Fig. 4 for different powers and Fig. 5 for different times. The origin of the grooves seen in Fig. 4 may lie in discontinuities in the lattice, such as grain boundaries or defects originating in the bulk material that reach the surface, *i.e.* dislocations. We have found a strong correlation between the grooves encountered in the images (such as that in Fig. 8a and others in longer scan size images, not shown here) and the grain borders detected in HOPG by the electron channeling micrograph (ECM) technique,[48] both seeming to occur with the same frequency. Also, it is always

seen that, in the case of pit and groove formation, the reaction progresses preferentially along directions parallel to the basal plane, as has been noted by other authors,[49] and this is because the oxygen atoms combine more easily with carbon atoms with dangling bonds, *i.e.* those from the basal plane edges.

As seen in Fig. 7, the etching along steps seems to be preferentially localized in specific areas, around which pits of several sizes develop. The formation of pits along steps, and also in the basal planes, with extended etching times has its roots in the selectivity of the chemical etching referred to previously. This can be explained by the presence of atomic vacancies that exist in the starting material or which were formed at different times during the etching by abstraction of carbon atoms, so the pits developed would have different sizes.[49] The abstraction of carbon atoms would be easier along a discontinuity, such as a step, so the number of pits formed in those areas should be greater. Likewise, it was previously mentioned that the reaction along steps progressed more rapidly at higher steps. This can be due to a cooperative effect, previously observed in graphite exposed to molecular oxygen,[17,27,50] which Stevens and Beebe[51] attribute to an interaction between the stacked HOPG edges. More recently, following a theoretical atomistic study of the reaction of O_2 molecules with graphite, Lee *et al.*[52] have suggested that the CO desorbed from low-lying layers of a multilayer edge can collide with an oxygen atom adsorbed on a higher layer, facilitating the removal of volatile species. This effect can also apply in the present case of an oxygen plasma.

The origin of the rough and disordered features in plasma-treated HOPG can be found in the way the oxygen atoms attack the surface. These progressively transform the atomically flat surface into a rough one when CO and CO_2 desorb from functional groups formed in this attack,[11] leaving atomic vacancies on the surface which, in turn, favour the chemisorption of more oxygen atoms and then the departure of more carbon atoms as CO or CO_2. Although the energy of the impinging ions is low enough not to create defects on the HOPG surface, as noted previously, it may be high enough to assist the desorption of the functional groups created by the chemical reactions, albeit to a much lesser extent than, for example, the RF case. Moreover, different functional groups formed on the surface may desorb with somewhat different energies, thus taking carbon atoms away from the surface at different rates. Likewise, the different activation energies of zig-zag and armchair-like sites[16] may contribute to the configuration of the features formed on the surface (Fig. 2).

As mentioned previously, the density of reactive species, *i.e.* oxygen atoms, in the plasma increases with MW power, so a more intense chemical etching over the surface is to be expected at higher powers. Thus, the large number of hillocks with a considerable height observed in the sample treated at 50 W (Fig. 2a) evolve into blunt protuberances when the MW power is increased to 250 W (Fig. 2c), due to the greater etching by oxygen atoms at the exposed tops of the hillocks, which limits the development of high isolated peaks but promotes the merging of the hillocks instead. This can be further appreciated in the power spectral density (PSD) calculations of the surfaces treated at different powers, which are presented in Fig. 9. The PSD calculations, based on a two-dimensional fast Hartley transform (FHT) and an angular mean value,[53] show that the higher MW powers progressively reduce the contribution of high and medium frequencies and increase slightly that of low frequencies, consistent with the disappearance of isolated peaks and their evolution to merging hillocks.

As for the evolution of topography with etching time, the differences between several areas of the samples accentuate with increasing treatment time because the oxidation will be favoured at certain points from the outset due to the existence of surface defects (present in the pristine material or created by the plasma at very early stages) where the reaction evolves at a

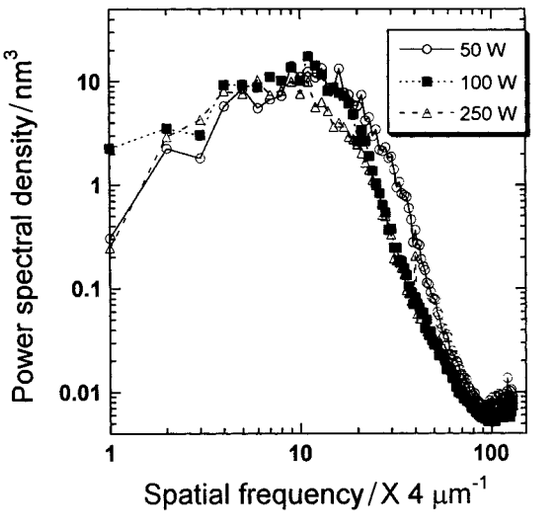

Fig. 9 Plot of the power spectral density *versus* spatial frequency for the HOPG samples treated at different powers for 5 min.

different rate. This could explain the formation of pits of considerable size after 20 min of treatment (Fig. 7). The development of pits of increasing size is a constant in treatments for increasing time and is in contrast to areas where the oxidation has progressed at a slower pace. Likewise, it can be seen from Fig. 5 and 6 that the etching was more important in the sample treated for 20 min than in all the others, but to a rather greater extent than one would expect looking at the samples treated for 5, 10 and 15 min. The lack of an energetic ion bombardment can explain the slow etching rate at short times. However, at longer treatment times there could be a rise in the substrate temperature that would facilitate the desorption of functional groups, thereby increasing the etching rate, at least to some extent. Dzioba *et al.*[47] observed an increase in the rate of resist stripping due to a rise in the substrate temperature in a downstream MW oxygen plasma. To clarify this point, we measured the substrate temperature in the plasma at given treatment times. Since a thermocouple cannot be used in our case, due to the type of reactor employed and also because it could modify the MW field, we used some special white strips (Testo GmbH, Germany) which turn black when the temperature reaches a certain value. Thus, the substrate temperature reached 130 °C for a 5 min etching time and about 190 °C for a 20 min experiment. This is consistent with the observation made by Ismail and Walker[54] of a significant increase in carbon gasification rates by O_2 (due to higher desorption rates) above a temperature of 177 °C in chars.

5 Conclusions

Atomic force microscopy has proved to be a valuable tool for the study of the surface topography of plasma-treated HOPG under different experimental conditions. After etching, the surfaces present a rough topography with nanometer-sized hillocks, in contrast to the atomically flat surfaces of the pristine material. The attack is dominated by chemical reactions between oxygen atoms from the plasma and carbon atoms from the substrate, the ion bombardment playing a minor role in the etching. This results in a chemical selectivity, as noticed in the presented images, that leads to etching differences between defect areas and perfect sites of basal planes. In particular, the observed grooves develop from grain borders in the HOPG. The evolution of the topography with increasing plasma power is due to the more intense chemical etching of oxygen atoms at higher plasma powers, which prevents the formation of isolated hillocks. With extended

etching times, the formation of pits of a considerable size has its roots in the different reactivities of defects (present in the fresh material or created by the plasma) compared with perfect sites, which amplifies with time. Likewise, a temperature effect may be responsible for the significant increase in etching observed in the 20 min sample. A greater reactivity in directions parallel to the basal planes compared with that along the *c* axis was also reported.

Acknowledgements

J. I. Paredes is indebted to the FICYT for fellowship support. Financial support from DGICYT (grants APC96-0012 and PB98-0492) and CICYT (grant MAT96-0430) is gratefully acknowledged.

References

1 M. A. Lieberman and A. J. Lichtenberg, *Principles of Plasma Discharges and Materials Processing*, John Wiley and Sons, New York, 1994, ch. 9.
2 C. M. Chan, T. M. Ko and H. Hiraoka, *Surf. Sci. Rep.*, 1996, **24**, 1.
3 E. M. Liston, *J. Adhes.*, 1989, **30**, 199.
4 J. W. Connell, J. G. Smith, C. G. Kalil and E. J. Siochi, *Polym. Adv. Technol.*, 1998, **9**, 11.
5 P. Pattabiraman, N. M. Rodriguez, B. Z. Jang and R. T. K. Baker, *Carbon*, 1990, **28**, 867.
6 T. Yamashina and T. Hino, *Appl. Surf. Sci.*, 1991, **48–49**, 483.
7 R. Moormann, H. K. Hinssen, A.-K. Krüssenberg, B. Stauch and C. H. Wu, *J. Nucl. Mater.*, 1994, **212–215**, 1178.
8 E. Taglauer, B. M. U. Scherzer, P. Varga, R. Behrisch, C. C. Kai and ASDEX-Team, *J. Nucl. Mater.*, 1982, **111–112**, 142.
9 K. Ashida, K. Kanamori, M. Matsuyama and K. Watanabe, *J. Nucl. Mater.*, 1986, **136**, 284.
10 X. Lu, H. Huang, N. Nemchuk and R. S. Ruoff, *Appl. Phys. Lett.*, 1999, **75**, 193.
11 M. Nakahara and Y. Sanada, *J. Mater. Sci.*, 1994, **29**, 3193.
12 M. Nakahara and Y. Sanada, *J. Mater. Sci.*, 1995, **30**, 4363.
13 M. J. Nowakowski, J. M. Vohs and D. A. Bonnell, *Surf. Sci.*, 1992, **271**, L351.
14 J. Fournier, D. Miousse, L. Brossard and H. Menard, *Mater. Chem. Phys.*, 1995, **42**, 181.
15 A. Dunlop, G. Jaskierowicz and L. T. Chadderton, *Nucl. Instrum. Methods Phys. Res., Sect. B*, 1998, **145**, 532.
16 H. X. You, N. M. D. Brown and K. F. Al-Assadi, *Surf. Sci.*, 1993, **284**, 263.
17 X. Chu and L. D. Schmidt, *Carbon*, 1991, **29**, 1251.
18 X. Chu and L. D. Schmidt, *Surf. Sci.*, 1992, **268**, 325.
19 H. Chang and A. J. Bard, *J. Am. Chem. Soc.*, 1991, **113**, 5588.
20 A. A. Gewirth and A. J. Bard, *J. Phys. Chem.*, 1988, **92**, 5563.
21 D. Tandon, E. J. Hippo, H. Marsh and E. Sebok, *Carbon*, 1997, **35**, 35.
22 K. G. Vandervoort, K. N. McLain and D. J. Butcher, *Appl. Spectrosc.*, 1997, **51**, 1896.
23 A. Tracz, G. Wegner and J. P. Rabe, *Langmuir*, 1993, **9**, 3033.
24 A. Tracz, A. A. Kalachev, G. Wegner and J. P. Rabe, *Langmuir*, 1995, **11**, 2840.
25 Z. Klusek, *Appl. Surf. Sci.*, 1998, **125**, 339.
26 S. G. Hall, M. B. Nielsen and R. E. Palmer, *J. Appl. Phys.*, 1998, **83**, 733.
27 S. Stevens, L. A. Kolodny and T. P. Beebe, *J. Phys. Chem. B*, 1998, **102**, 10799.
28 N. Chen, R. T. Yang and R. S. Goldman, *J. Catal.*, 1998, **180**, 245.
29 K. Mochiji, S. Yamamoto, H. Shimizu, S. Ohtani, T. Seguchi and N. Kobayashi, *J. Appl. Phys.*, 1997, **82**, 6037.
30 J. R. Hahn, H. Kang, S. Song and I. C. Jeon, *Phys. Rev. B*, 1996, **53**, R1725.
31 N. Almqvist, M. Rubel, S. Frediksson, B. Emmoth, P. Wienhold and L. Ilyinski, *J. Nucl. Mater.*, 1995, **220–222**, 917.
32 M. Kappel, M. Steidl, J. Biener and J. Küppers, *Surf. Sci.*, 1997, **387**, L1062.
33 Q. Zhao, H. Yi Lu and D. W. Hess, *J. Electrochem. Soc.*, 1996, **143**, 2896.
34 Q. Zhong, D. Inniss, K. Kjoller and V. B. Elings, *Surf. Sci.*, 1993, **290**, L688.
35 J. Tamayo and R. Garcia, *Langmuir*, 1996, **12**, 4430.
36 S. N. Magonov, J. Cleveland, V. Elings, D. Denley and M.-H. Whangbo, *Surf. Sci.*, 1997, **389**, 201.
37 M. A. Hartney, D. W. Hess and D. S. Soane, *J. Vac. Sci. Technol., B*, 1989, **7**, 1.
38 H. F. Winters, *J. Vac. Sci. Technol., A*, 1988, **6**, 1997.
39 D. L. Flamm, in *Plasma Etching*, ed. D. M. Manos and D. L. Flamm, Academic Press, San Diego, 1989, ch. 2.
40 L. Holland, *J. Vac. Sci. Technol.*, 1977, **14**, 5.
41 J. W. Coburn, *J. Vac. Sci. Technol., A*, 1994, **12**, 1417.
42 M. R. Wertheimer and M. Moisan, *J. Vac. Sci. Technol., A*, 1985, **3**, 2643.
43 J. Paraszczak and J. Heidenreich, in *Microwave Excited Plasmas*, ed. M. Moisan and J. Pelletier, Elsevier, Amsterdam, 1992, ch. 15.
44 D. Marton, H. Bu, K. J. Boyd, S. S. Todorov, A. H. Al-Bayati and J. W. Rabalais, *Surf. Sci.*, 1995, **326**, L489.
45 F. D. Egitto, F. Emmi, R. S. Horwath and V. Vukanovic, *J. Vac. Sci. Technol., B*, 1985, **3**, 893.
46 W. P. Hoffman, *Carbon*, 1992, **30**, 315.
47 S. Dzioba, G. Este and H. M. Naguib, *J. Electrochem. Soc.*, 1982, **129**, 2537.
48 A. Yoshida and Y. Hishiyama, *J. Mater. Res.*, 1992, **7**, 1400.
49 C. Wong, R. T. Yang and B. L. Halpern, *J. Chem. Phys.*, 1983, **78**, 3325.
50 E. L. Evans, R. J. M. Griffiths and J. M. Thomas, *Science*, 1971, **171**, 174.
51 F. Stevens and T. P. Beebe, *Comput. Chem.*, 1999, **23**, 175.
52 S. M. Lee, Y. H. Lee, Y. G. Hwang, J. R. Hahn and H. Kang, *Phys. Rev. Lett.*, 1999, **82**, 217.
53 S. J. Fang, S. Haplepete, W. Chen, C. R. Helms and H. Edwards, *J. Appl. Phys.*, 1997, **82**, 5891.
54 I. M. K. Ismail and P. L. Walker, *Carbon*, 1989, **27**, 549.